Received: 23 March 2020 | Accepted: 31 March 2020

DOI: 10.1002/pld3.219

ORIGINAL RESEARCH

Hydroxyl carlactone derivatives are predominant strigolactones in *Arabidopsis*

Kaori Yoneyama[1,2] | Kohki Akiyama[3] | Philip B. Brewer[4] | Narumi Mori[3] | Miyuki Kawano-Kawada[1] | Shinsuke Haruta[1] | Hisashi Nishiwaki[1] | Satoshi Yamauchi[1] | Xiaonan Xie[5] | Mikihisa Umehara[6] | Christine A. Beveridge[7] | Koichi Yoneyama[5,8] | Takahito Nomura[5]

[1]Graduate School of Agriculture, Ehime University, Matsuyama, Japan

[2]Japan Science and Technology, PRESTO, Kawaguchi, Japan

[3]Department of Applied Life Sciences, Graduate School of Life and Environmental Sciences, Osaka Prefecture University, Sakai, Japan

[4]ARC Centre of Excellence in Plant Energy Biology, School of Agriculture, Food and Wine, The University of Adelaide, Adelaide, SA, Australia

[5]Center for Bioscience Research and Education, Utsunomiya University, Utsunomiya, Japan

[6]Department of Applied Biosciences, Faculty of Life Sciences, Toyo University, Gunma, Japan

[7]ARC Centre of Excellence for Plant Success in Nature and Agriculture, School of Biological Sciences, The University of Queensland, St. Lucia, QLD, Australia

[8]Women's Future Development Center, Ehime University, Matsuyama, Japan

Correspondence
Kaori Yoneyama, Graduate School of Agriculture, Ehime University, Matsuyama, Japan.
Email: yoneyama.kaori.wx@ehime-u.ac.jp

Funding information
Japan Science and Technology Research Promotion Program for Agriculture, Forestry, Fisheries and Food Industry; Japan Society for the Promotion of Sciences, Grant/Award Number: 15K07093, 16K07618, 16K18560 and 17K07650; Japan Science and Technology Agency, Grant/Award Number: JPMJPR17QA; Australian Research Council, Grant/Award Number: DP110100808 and FT180100081

Abstract

Strigolactones (SLs) regulate important aspects of plant growth and stress responses. Many diverse types of SL occur in plants, but a complete picture of biosynthesis remains unclear. In *Arabidopsis thaliana*, we have demonstrated that MAX1, a cytochrome P450 monooxygenase, converts carlactone (CL) into carlactonoic acid (CLA) and that LBO, a 2-oxoglutarate-dependent dioxygenase, can convert methyl carlactonoate (MeCLA) into a metabolite called [MeCLA + 16 Da]. In the present study, feeding experiments with deuterated MeCLAs revealed that [MeCLA + 16 Da] is hydroxymethyl carlactonoate (1'-HO-MeCLA). Importantly, this LBO metabolite was detected in plants. Interestingly, other related compounds, methyl 4-hydroxycarlactonoate (4-HO-MeCLA) and methyl 16-hydroxycarlactonoate (16-HO-MeCLA), were also found to accumulate in *lbo* mutants. 3-HO-, 4-HO-, and 16-HO-CL were detected in plants, but their expected corresponding metabolites, HO-CLAs, were absent in *max1* mutants. These results suggest that HO-CL derivatives may be predominant SLs in *Arabidopsis*, produced through MAX1 and LBO.

KEYWORDS

Arabidopsis thaliana, hydroxyl carlactone derivative, lateral branching oxidoreductase

1 | INTRODUCTION

Strigolactones (SLs) were originally identified as germination stimulants for root parasitic plants (Cook, Whichard, Turner, Wall, & Egley, 1966) and then as hyphal branching factors for symbiotic arbuscular mycorrhizal (AM) fungi (Akiyama, Matsuzaki, & Hayashi, 2005). SLs were thought to function only as rhizosphere signals until the discovery of their role as a plant hormonal signal that inhibits lateral shoot branching (Gomez-Roldan et al., 2008;Umehara et al., 2008).

Shoot branching involves the formation of axillary buds in the axil of leaves. The level of dormancy in buds is an essential determinant of plant architecture. Defects in the SL pathway correspond with loss of bud dormancy and excessive shoot branching as displayed by SL mutants that include *ramosus* (*rms*) of pea (*Pisum sativum*), *decreased apical dominance* (*dad*) of petunia (*Petunia hybrida*), *dwarf* (*d*) of rice (*Oryza sativa*), and *more axillary growth* (*max*) of *Arabidopsis* (*Arabidopsis thaliana*).

Natural SLs are carotenoid-derived compounds consisting of a butenolide D ring linked by an enol-ether bridge to a less conserved moiety. These SLs can be classified into two structurally distinct groups: canonical and non-canonical SLs. Canonical SLs contain the ABCD ring formation, and non-canonical SLs lack the A, B, or C ring but have the enol-ether–D ring moiety (Al-Babili & Bouwmeester, 2015). During biosynthesis, the initial compound that contains the D ring is carlactone (CL), an endogenous precursor for SLs, which is produced by the sequential reactions of 9-*cis*/all-*trans*-β-carotene isomerase and two carotenoid cleavage dioxygenases (CCD7, CCD8) (Alder et al., 2012). In *Arabidopsis*, the isomerase is encoded by *DWARF27* (*D27*), and CCD7 and CCD8 by *MAX3* and *MAX4*, respectively (Figure 1). We have demonstrated that recombinant MAX1, (a cytochrome P450 monooxygenase) expressed in yeast, converts CL to carlactonoic acid (CLA) by oxidations at C-19 (Abe et al., 2014). This function was also observed in MAX1 homologs of other plant species including rice, maize, tomato, a model tree poplar, and a lycophyte spike moss, suggesting this conversion of CL to CLA is highly conserved in the plant kingdom (Yoneyama et al., 2018). It was also shown that CL, CLA, and methyl carlactonoate (MeCLA) are present in *Arabidopsis* root tissues (Abe et al., 2014;Seto et al., 2014). Furthermore, differential scanning fluorimetry and hydrolysis activity tests showed that, among CL, CLA, and MeCLA, only MeCLA could interact with the SL receptor, AtD14, suggesting MeCLA may be biologically active in the inhibition of shoot branching in *Arabidopsis* (Abe et al., 2014). *Arabidopsis max1* mutants display a highly increased lateral shoot branching phenotype and yet accumulate CL (Seto et al., 2014), indicating that CL is not active in repressing shoot branching.

As a novel SL biosynthetic gene, *LATERAL BRANCHING OXIDOREDUCTASE* (*LBO*), encoding a 2-oxoglutarate and Fe (II)-dependent dioxygenase, was identified by using a transcriptomic approach and was shown to function downstream of MAX1 (Brewer et al., 2016). *Arabidopsis lbo* mutant shoot branching is increased compared to WT (Ws-4), but its phenotype is intermediate between WT and *max4* mutants. LC-MS/MS analysis of SLs revealed that CL and MeCLA accumulate in root tissues of *lbo* mutants (Brewer et al., 2016). Because the active shoot branching inhibitor MeCLA accumulates in *lbo* mutants, the intermediate branching phenotype of *lbo* mutants might be explained by the presence of MeCLA. Thus, it was suggested that LBO is necessary for complete suppression of shoot branching in plants by converting the partly bioactive MeCLA to a compound with greater bioactivity for branching. We then showed that the LBO enzyme expressed in *E. coli* only consumed MeCLA when fed with CL, CLA, or MeCLA and converted MeCLA into a product of [MeCLA + 16 Da]. However, complete characterization of this LBO metabolite had not yet been conducted.

In the present study, we have determined the structure of the [MeCLA + 16 Da] compound produced by LBO from MeCLA by feeding experiments using deuterated MeCLAs. In addition, we could identify this LBO metabolite as an endogenous compound from not only roots, but also basal parts of *Arabidopsis* shoot tissues. Since two additional *lbo* mutant alleles, *lbo-2* and *lbo-3*, exist, and homozygous mutant plants exhibited increased shoot branching (Brewer et al., 2016), recombinant proteins of LBO-2 and LBO-3 were produced and the correlation between their enzymatic activities in the conversion of MeCLA to [MeCLA + 16 Da] and their shoot branching phenotypes was investigated to further estimate the importance of the LBO metabolite for shoot branching. Then, biochemical functions of LBO homologs in other plant species including tomato, maize, and sorghum were examined to clarify whether the conversion of MeCLA to [MeCLA + 16 Da] is conserved among these plant species. Furthermore, endogenous SLs in *Arabidopsis max1* and *lbo* mutants were carefully analyzed in search of other potential substrates for MAX1 and LBO to better understand the SL biosynthetic pathway in *Arabidopsis*.

2 | MATERIALS AND METHODS

2.1 | Plant materials

The *lbo-1* and *max1-4* were from our *Arabidopsis* laboratory stocks (Brewer et al., 2016), and the *atd14-2* mutant was obtained from a TILLING project in the Columbia-0 (Col-0) ecotype. To extract total RNAs, tomato (cv Ailisa Craig; (Nomura et al., 2005), maize (cv B73; Yoneyama et al., 2018), and sorghum (cv Hybrid; Yoneyama et al., 2008) were used.

2.2 | Chemicals

3-, 4-, and 18-HO-CLs were synthesized as described previously (Baz et al., 2018;Mori, Nishiuma, Sugiyama, Hayashi, & Akiyama, 2016). 2- and 16-HO-CLs were synthesized using the same strategy as the synthesis of 3- and 18-HO-CLs (Baz et al., 2018;Mori et al., 2016). The detailed synthesis will be published elsewhere. 2-, 3-, 4-, 16-, and 18-HO-CLA were obtained by MAX1 microsome assay using

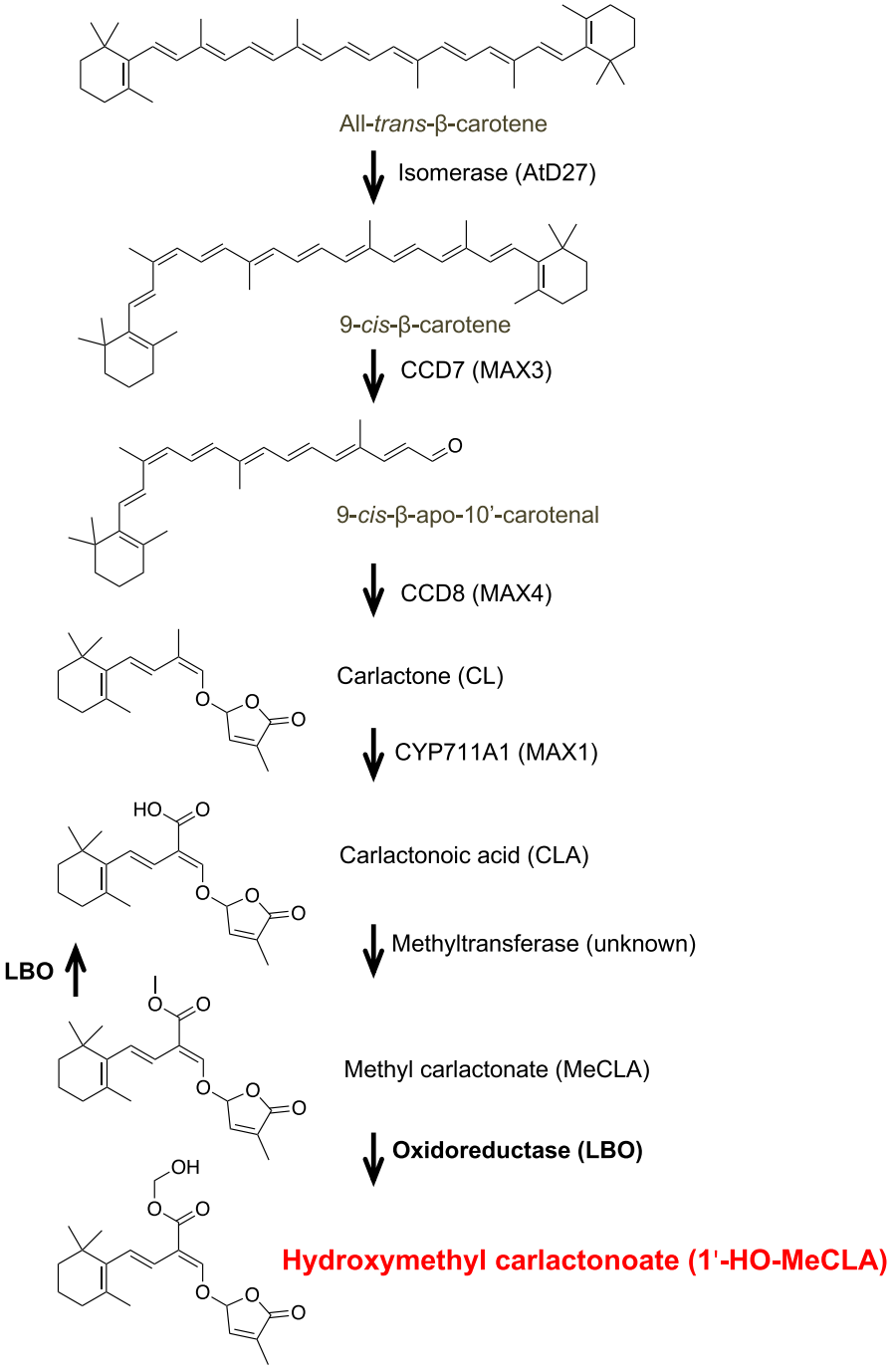

FIGURE 1 Proposed strigolactone (SL) biosynthesis pathway in *Arabidopsis*. An isomerase (AtD27) and two CCD enzymes (MAX3 and MAX4) convert β-carotene into carlactone (CL), an endogenous common precursor for diverse SLs. CL is then oxidized by cytochrome P450 (MAX1) to carlactonoic acid (CLA), which is converted into MeCLA by unknown methyltransferase. The present study shows that 2-oxoglutarate-dependent-dioxygenase LBO can convert MeCLA into 1'-HO-MeCLA, suggesting that 1'-HO-MeCLA may regulate shoot branching

the corresponding HO-CLs. For this, MAX1 expressed in yeast (*Saccharomyces cerevisiae*) was prepared as described previously (Abe et al., 2014;Yoneyama et al., 2018). 2-, 3-, 4-, 16-, and 18-HO-MeCLA were prepared by methylation of the corresponding HO-CLAs with diazomethane.

2.3 | Synthesis of methyl-d_3 carlactonoate (1'-d_3-MeCLA) (Scheme S1)

(*E*)-4-(2,6,6-Trimethylcyclohex-1-en-1-yl)but-3-enoic acid was synthesized as reported (Abe et al., 2014). To a solution of the C_{13}-carboxylic acid (88.1 mg, 0.42 mmol) in acetone (2 ml), K_2CO_3 (174 mg, 1.26 mmol) and methyl-d_3 iodide (305 mg, 131 µl, 2.1 mmol) were added. The mixture was stirred at room temperature for 21 hr under argon. After being concentrated under nitrogen gas flow, the residue was dissolved with ether and water. The organic phase was washed with water and dried over $MgSO_4$. Filtration and evaporation of the solvent afforded C_{13}-carboxylic acid methyl-d_3 ester (82.3 mg, 0.37 mmol, 87%), which was pure enough for the next reaction. Ester condensation of the methyl-d_3 ester (82.3 mg, 0.37 mmol) with ethyl formate (98 mg, 106 µl, 1.32 mmol) by the use of sodium hydride (13.3 mg, 0.56 mmol) in *N*,*N*-dimethylformamide (1 ml) followed by alkylation with racemic 4-bromo-2-methyl-2-buten-4-olide (99 mg, 55 µl, 0.56 mmol) (Abe

et al., 2014) provided 1'-d_3-MeCLA and ethyl carlactonoate (EtCLA, a transesterification product). Purification by silica gel column chromatography (Kieselgel 60, Merck, *n*-hexane-ethyl acetate stepwise) and semi-preparative HPLC (Inertsil SIL-100A, GL Sciences, 5% ethanol in *n*-hexane) gave 1'-d_3-MeCLA (2.5 mg, 0.0072 mmol, 1.9%). **1'-d_3-MeCLA**: HR-ESI-TOF-MS *m/z*: 372.1855 $[M + Na]^+$ (calcd. for $C_{20}H_{23}D_3NaO_5^+$, *m/z*: 372.1861).

2.4 | Synthesis of methyl 18- d_3-carlactonoate (18-d_3-MeCLA) (Scheme S2)

6,6-Dimethyl-2-(methyl-d_3)cyclohex-1-en-1-yl trifluoromethanesulfonate was synthesized as reported (Tanaka et al., 2007). A mixture of the triflate (5.30 g, 19.3 mmol), triethylamine (7.80 g, 10.7 ml, 77.2 mmol), methyl 3-butenoate (3.86 g, 4.11 ml, 38.6 mmol), and bis(triphenylphosphine)palladium(II) dichloride (1.35 g, 1.92 mmol) in *N*,*N*-dimethylformamide (50 ml) was stirred at 100°C for 17 hr under argon. The reaction mixture was cooled, quenched by pouring into 1 N HCl, and extracted with ether. The organic phase was washed with brine and water, dried over $MgSO_4$, and concentrated in vacuo. Purification by silica gel column chromatography (Kieselgel 60, Merck, *n*-hexane-ether stepwise) gave crude methyl (*E*)-4-(6,6-dimethyl-2-(methyl-d_3)cyclohex-1-en-1-yl)but-3-enoate (1.31 g, 5.8 mmol, 30%), which was used for the next reaction without further purification. Ester condensation of the deuterium-labeled ester (108 mg, 0.48 mmol) with methyl formate (86.4 mg, 89 µl, 1.44 mmol) by the use of sodium hydride (11.5 mg, 0.48 mmol) in *N*,*N*-dimethylformamide (1 ml) followed by alkylation with racemic 4-bromo-2-methyl-2-buten-4-olide (85 mg, 47 µl, 0.48 mmol) (Abe et al., 2014) provided 18-d_3-MeCLA. Purification by silica gel column chromatography (Kieselgel 60, Merck, *n*-hexane-ethyl acetate stepwise), semi-preparative normal-phase HPLC (Inertsil SIL-100A, GL Sciences, 5% ethanol in *n*-hexane), and semi-preparative reversed-phase HPLC (InertSustain C18, GL Sciences, 85% acetonitrile in water) gave 18-d_3-MeCLA (1.7 mg, 0.0049 mmol, 1.0%). **18-d_3-MeCLA**: HR-ESI-TOF-MS *m/z*: 350.2058 $[M + H]^+$ (calcd. for $C_{20}H_{24}D_3O_5^+$, *m/z*: 350.2041).

2.5 | Cloning

The primer sequences used are listed in Supporting Information Table S1. Total RNAs were extracted from the shoots and roots of plant materials using an RNeasy Plant Mini Kit (Qiagen) and employed to synthesize single-strand cDNAs by a SuperScript III First-Strand Synthesis System (Invitrogen). PCR amplification was performed using PrimeSTAR HS DNA polymerase (TAKARA Bio Inc.) with/without GC buffer for accurate amplification of GC rich targets. The full-length cDNAs were cloned into the pENTR vector and then transferred to pET300 vector by the Gateway system (Invitrogen). Recombinant plasmid DNA was transferred to *Escherichia coli* strain Rosetta 2(DE3)pLysS (Novagen). At least four colonies for each experiment were sequenced to check for errors in the PCR. Sequence alignment was performed using MAC VECTOR software (Mac Vector Inc.).

2.6 | Heterologous expression in *E. coli*

Heterologous expression of LBO in *E. coli* was carried out as described previously (Brewer et al., 2016). Briefly, transformed colonies were grown in LB media (0.5% yeast extract, 1% Bacto Tryptone, 1% NaCl) with carbenicillin (100 µg/ml) at 37°C in a shaking incubator (180 rpm) until the cell density reached an OD_{600} of 0.5–0.8. After isopropyl -D-1-thiogalactopyranoside (1 mM) was added, transformed *E. coli* were incubated at 20°C for 14–16 hr. To prepare enzyme fractions, *E. coli* cells were collected by centrifugation of 10,000 *g* for 1 min and suspended in 20 mM phosphate buffer (pH 7.4). The suspend cells were mechanically lysed by using a high-pressure homogenizer (Emulsi Flex B15; AVESTIN) and then centrifuged at 15,000 *g* for 5 min at 4°C.

2.7 | LBO enzyme assays and metabolite extraction

Crude protein fraction (5 ml) was incubated with 4 mM 2-oxoglutarate, 0.5 mM iron ascorbate, 5 mM ascorbic acid, and 12.5 µg of test substrates at 27°C for 20 min, similar to the previous report (Brewer et al., 2016). The reaction mixture was extracted with 5 ml ethyl acetate twice. The ethyl acetate soluble fraction was dried with Na_2SO_4 and evaporated under nitrogen gas flow at 40°C with care not to completely dry. Crude extract samples were kept at –20°C until LC-MS analysis.

2.8 | SL identification in *A. thaliana*

Arabidopsis seeds were sterilized in 1% NaClO solution for 10 min and rinsed with sterile water. Seeds were sown on agar (0.5% gellangum with 1/2 Murashige and Skoog medium and 1% sucrose), stratified at 4°C for 2 days, and grown for 10 days under a photoperiod, 14 hr:10 hr, light (150 mol m^{-2} s^{-1}):dark, at room temperature. Then, healthy and uniform seedlings were transplanted on soils [horticultural soil: vermiculite = 1:2 (v/v)] and further grown until branching phenotype became clear. Basal parts of shoot tissues were harvested and extracted with ethyl acetate for at least 2 days, and crude extracts were purified by DEA and silica Sep-pack cartridge as reported previously (Brewer et al., 2016).

2.9 | LC-MS/MS analysis

SLs were analyzed by LC-MS/MS as reported previously (Abe et al., 2014). Briefly, LC-MS/MS analysis (MRM, multiple reaction monitoring and PIS, product ion scan) of proton adduct ions was performed with a triple quadruple/linear ion trap instrument (QTRAP5500; AB Sciex) with an electrospray source. HPLC

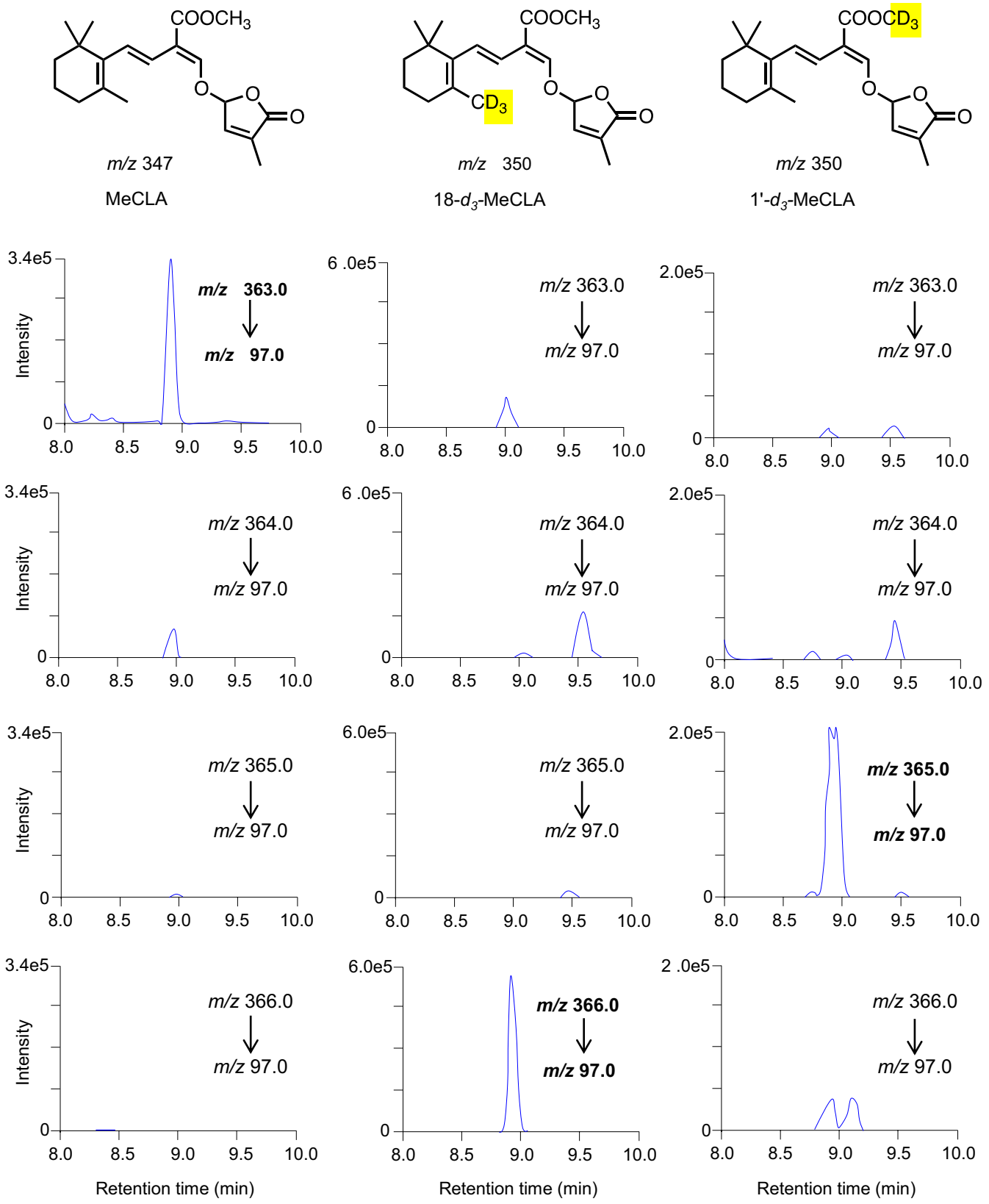

FIGURE 2 LBO converted 18-d_3-MeCLA to [MeCLA + 16+3] and 1'-d_3-MeCLA to [MeCLA + 16+2]. To characterize the structure of [MeCLA + 16], 18-d_3-MeCLA (*Middle*) and 1'-d_3-MeCLA (*Light*) were fed as substrates to recombinant LBO proteins and incubated for 15 min. Products were identified by LC-MS/MS (MRM)

separation was performed on a UHPLC (Nexera X2; Shimadzu) equipped with an ODS column (Kinetex C18, 2.1 × 150 mm, 1.7 m; Phenomenex) with a linear gradient of 35% acetonitrile (0 min) to 95% acetonitrile (20 min). The column oven temperature was maintained at 30°C.

3 | RESULTS

3.1 | LBO catalyzes the conversion of methyl carlactonoate (MeCLA) into hydroxymethyl carlactonoate (1'-HO-MeCLA)

To characterize the structure of [MeCLA + 16 Da], LBO enzyme reactions were performed repeatedly. Both the substrate MeCLA and the metabolite [MeCLA + 16 Da] were highly unstable, and the yield of the metabolite was extremely low. We tried to optimize enzyme assay conditions but the maximum yield of the LBO metabolite did not exceed 0.1%. Although more than 500 μg of synthetic MeCLA has been used for LBO enzyme assay, the amount of the metabolite after purification by DEA, silica, and HPLC was not enough for NMR spectroscopy measurement.

The observed mass of [MeCLA + 16 Da] (Brewer et al., 2016) suggests that LBO has simply added an oxygen to MeCLA. Therefore, feeding experiments using deuterated MeCLAs were conducted to identify the site of oxidation of MeCLA (Nomura et al., 2013). When MeCLA was fed to LBO, the metabolite was detected by the transition of *m/z* 363 to 97 (Figure 2). When 18-d_3-MeCLA was fed, the metabolite was detected by the transition of *m/z* 366 to 97 (Figure 2), clearly indicating that 18-d_3 remained unaffected, and thus, oxidation did not occur at C-18. By contrast, when 1'-d_3-MeCLA, in which the ester methyl group had been labeled with deuterium, was fed, a major metabolite was detected by the transition of *m/z* 365 to 97 (Figure 2), apparently showing that the ester methyl group was oxidized. Consequently, it was demonstrated that LBO converts MeCLA into hydroxymethyl carlactonoate (1'-HO-MeCLA) (Figure 1).

On the other hand, when MeCLA was incubated with LBO, most MeCLA was converted to CLA; the ratio of CLA to 1'-HO-MeCLA was 100:1 based on the peak areas in the LC-MS/MS chromatograms of LBO reaction products (Figure 3), indicating that the LBO protein assay mainly produces CLA.

3.2 | 1'-HO-MeCLA is present in *atd14* mutants but not in *lbo* mutants

It is important to clarify whether 1'-HO-MeCLA is an endogenous compound in plant tissues because there is a possibility that 1'-HO-MeCLA would only be produced in the heterologous expression system. Identification of 1'-HO-MeCLA was conducted using *atd14* mutant plants, because they lack a functional SL receptor and accumulate SLs due to negative feedback on the biosynthesis pathway. As a negative control, *lbo* mutant plants were also used. 1'-HO-MeCLA

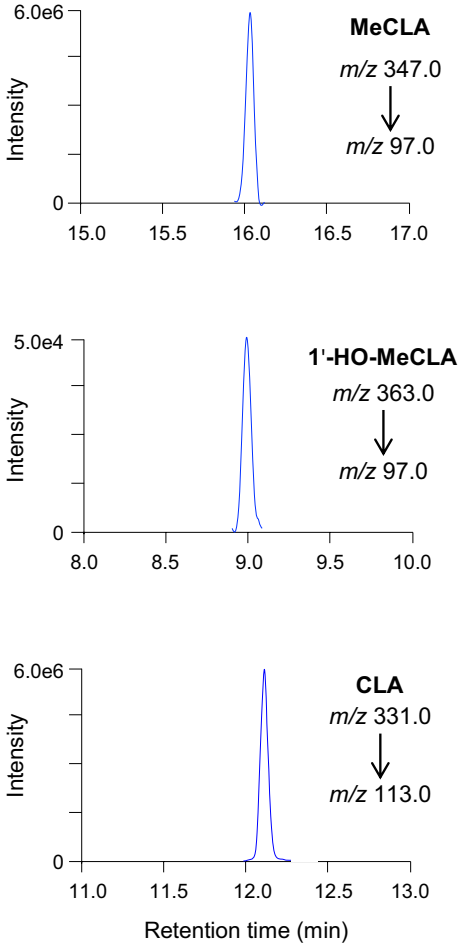

FIGURE 3 Most MeCLAs were converted to CLA. MeCLA was incubated with recombinant LBO proteins for 15 min. The extracts were analyzed by LC-MS/MS (MRM)

was detected from the basal part of shoots and also root tissues of *atd14* mutants (Figure 4). By contrast, CL and MeCLA, but not 1'-HO-MeCLA, were detected from both tissues of *lbo* mutants (Figure 4, Brewer et al., 2016). These results allow for the possibility that LBO acts to convert MeCLA into 1'-HO-MeCLA in plants.

3.3 | Production of 1'-HO-MeCLA correlates with shoot branching

We previously described additional alleles of mutation in the *LBO* gene (Brewer et al., 2016). *lbo-2* plants have a point mutation in the predicted catalytic domain and display significant extra branching. *lbo-3* plants have a point mutation elsewhere in the gene and have a branching phenotype that is much weaker than *lbo-2* (Brewer et al., 2016). LBO-2 and LBO-3 proteins were produced in the *E. coli* heterologous expression system, and enzymatic activities to produce 1'-HO-MeCLA were examined. The very low conversion of MeCLA to 1'-HO-MeCLA by LBO-2 enzyme activity (Figure 5) relates well to the mutant shoot branching phenotype. However, LBO-3 appears to have normal function in our assay (Figure 5).

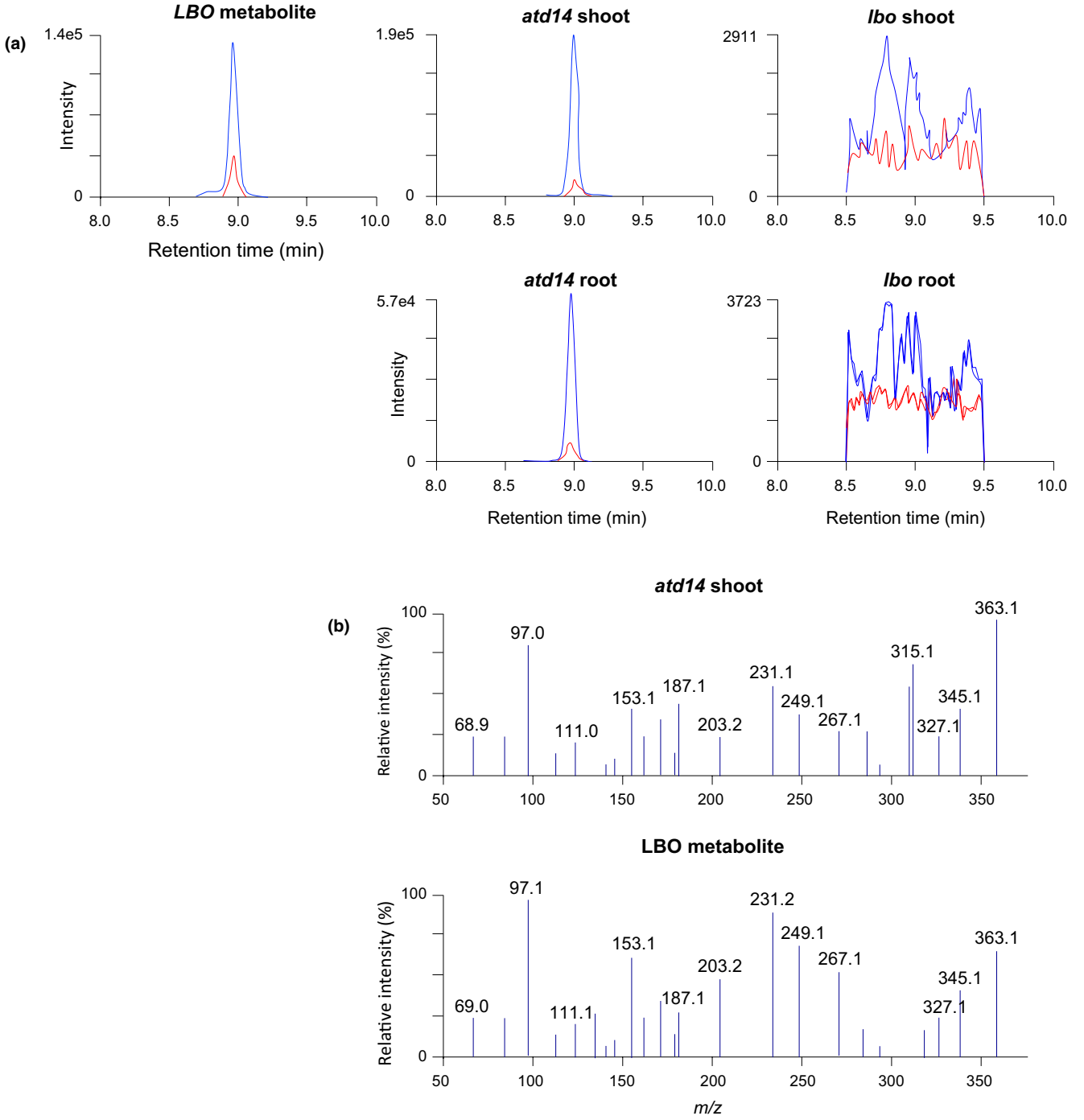

FIGURE 4 1'-HO-MeCLA was found from *atd14* shoot. Identification of endogenous 1'-HO-MeCLA in basal parts of shoot and root tissues was conducted. (a) MRM of chromatograms (blue, 363.0/97.0; red, 363.0/231.0; *m/z* in positive mode) of *atd14* mutants (*Middle*) and *lbo* mutants (*Light*). (b) Product ion spectra derived from endogenous 1'-HO-MeCLA in basal parts of shoot of *atd14* mutants

3.4 | Conversion of MeCLA into 1'-HO-MeCLA is conserved among different plant species

Tomato, maize, and sorghum have one LBO homolog each, and their recombinant LBO proteins were expressed in *E. coli*. Not only *Arabidopsis* LBO, but also the other LBO proteins examined, converted MeCLA into 1'-HO-MeCLA (Figure 6), where the major reaction product was CLA (Figure S1).

It is intriguing to test whether LBO has an ability to produce canonical SLs or not. Tomato plants produce canonical SLs such as solanacol and orobanchol. Tomato MAX1 expressed in yeast cannot produce canonical SLs from CL (Yoneyama et al., 2018). Accordingly, there is a possibility that tomato LBO produces canonical SLs including solanacol and orobanchol. However, tomato LBO produced neither solanacol nor orobanchol from MeCLA. In addition, tomato LBO did not convert 4DO into solanacol or orobanchol. Similar

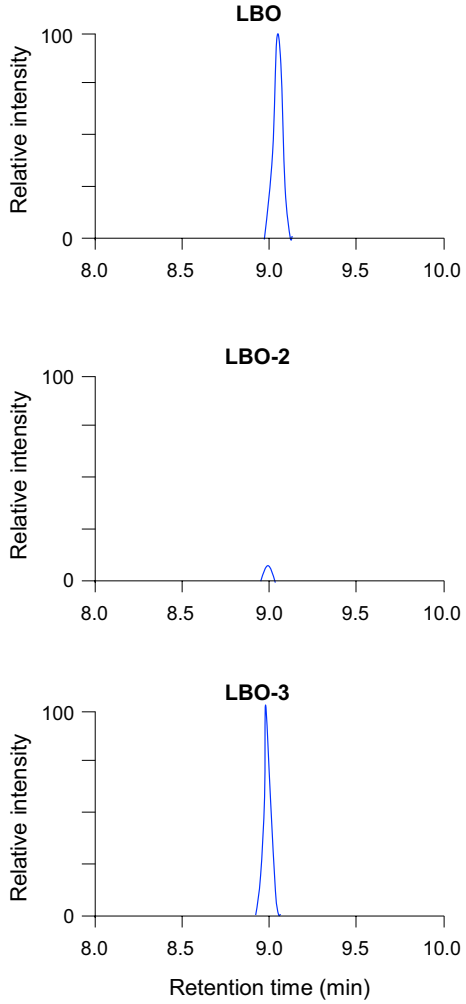

FIGURE 5 Production of 1'-HO-MeCLA is very low in LBO-2. MeCLA was incubated with each recombinant protein for 15 min, and extracts were analyzed by LC-MS/MS. MRM chromatograms of 1'-HO-MeCLA (363.0/97.0; *m/z* in positive mode) are shown

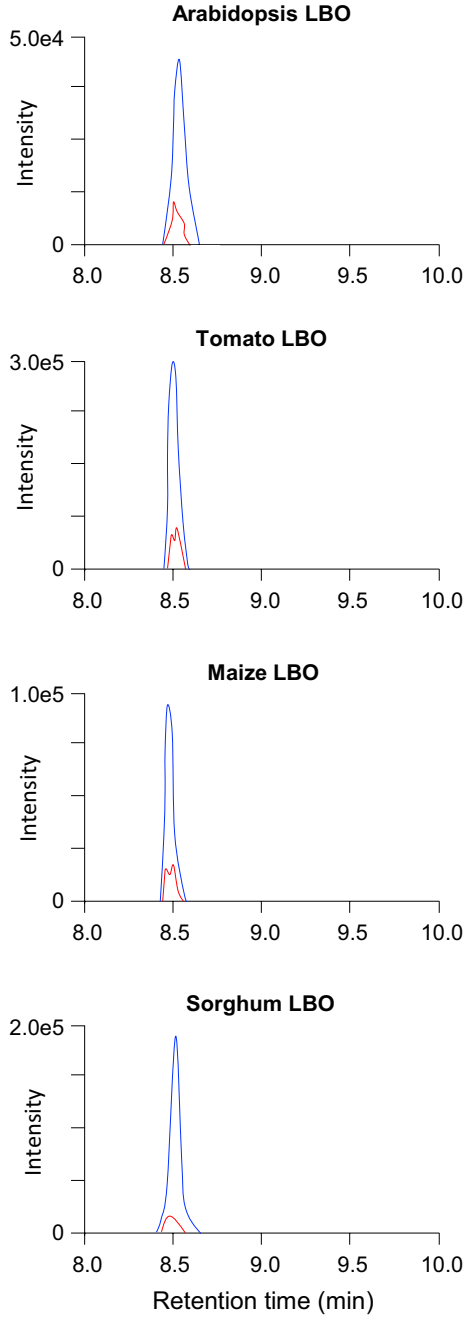

FIGURE 6 Conversion of MeCLA into 1'-HO-MeCLA is conserved among different plant species. MeCLA was incubated with each recombinant protein for 15 min, and extracts were analyzed by LC-MS/MS. MRM chromatograms of 1'-HO-MeCLA (blue, 363.0/97.0; red, 363.0/231.0; *m/z* in positive mode) are shown

results were obtained with sorghum or maize LBOs. Sorghum LBO produced neither 5-deoxystrigol (5DS) nor sorgomol, two major canonical SLs of sorghum (cv Hybrid), from MeCLA. Although it was proposed that sorgomol is produced from 5DS (Motonami et al., 2013), LBO did not produce sorgomol from 5DS. Maize plants produce zealactone (Charnikhova et al., 2017;Xie et al., 2017) and zeapyranolactone (Charnikhova et al., 2018), non-canonical SLs with unique structures. Maize LBO did not produce these SLs from MeCLA.

3.5 | Endogenous non-canonical SLs in *Arabidopsis*

CYP711A2, one of the rice MAX1 homologs, produces 4-deoxyorobanchol (4DO) via 18-HO-CLA from CL (Yoneyama et al., 2018). This suggests that not only 1'-HO-MeCLA but also other HO-CL derivatives including HO-CLs, HO-CLAs, and HO-MeCLAs are endogenous compounds in *Arabidopsis*, and some of them may be substrates for MAX1 and LBO. Therefore, endogenous SLs in *atd14*, *max1*, and *lbo* mutants were investigated in detail. Synthetic standards of 2-, 3-, 4-, 16-, and 18-HO-CL (Figure 7) were prepared and used for LC-MS/MS analyses. HO-CLAs (Figure 7) were obtained by conversion of the corresponding HO-CLs by MAX1 expressed in yeast. HO-MeCLAs (Figure 7) were obtained by methylation of the corresponding HO-CLAs with diazomethane.

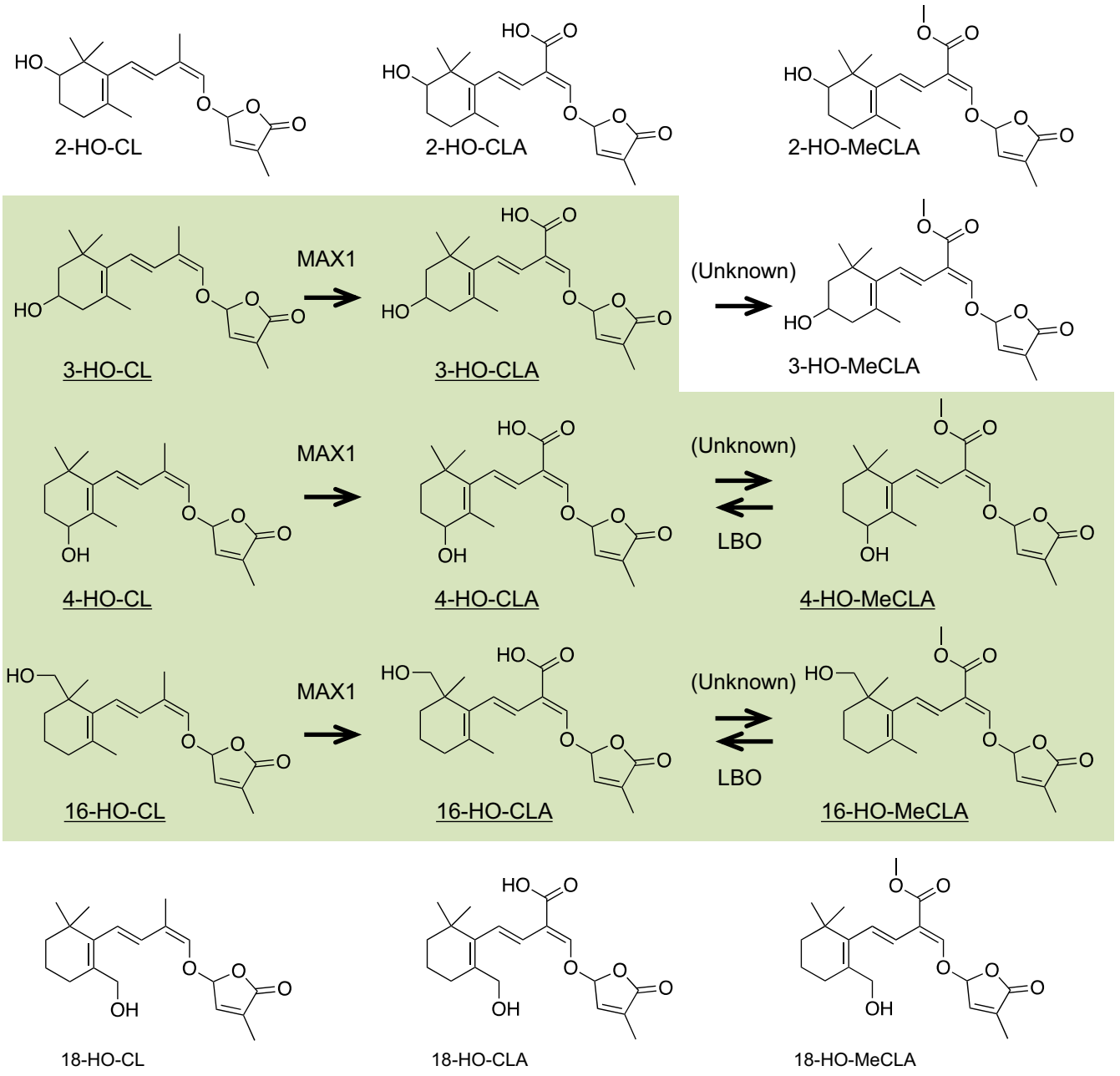

FIGURE 7 Structures of HO-CLs, HO-CLAs, and HO-MeCLAs and a proposed strigolactone biosynthesis pathway in *Arabidopsis*. The present study suggests that 3-, 4-, and 16-HO-CL derivatives are predominant and produced through MAX1 and LBO in *Arabidopsis*. Strigolactones in the green box were found from Arabidopsis tissues

Basal parts of *Arabidopsis* shoot were harvested when the shoot branching phenotype was clearly observed (Figure S2). From *atd14* mutants, 3-, 4-, and 16-HO-CLs, 3-, 4-, and 16-HO-CLAs, and 4- and 16-HO-MeCLAs, in addition to CL, CLA, and MeCLA, were detected (Figure 8).

3-, 4-, and 16-HO-CLs and CL were detected from basal parts of *max1* mutants (Figure 8). Although 3-, 4-, and 16-HO-CLAs were detected, even from Col-0 plants (Figure S3), these HO-CLAs were not detected in *max1* mutants (Figure 8). By comparing peak areas of MRM chromatograms between *atd14* and *max1* mutants (Figure 8), 3-, 4-, and 16-HO-CLs appeared to accumulate in *max1* mutants.

3.6 | 4- and 16-HO-MeCLAs are potential substrates for LBO

In addition to CL, CLA, and MeCLA, 16-HO-CL, 3-, 4-, 16-HO-CLAs, 4- and 16-HO-MeCLAs were found in *lbo* mutants (Figure 8). MeCLA was found to be a potential substrate for LBO (Brewer et al., 2016), and therefore, these HO-MeCLAs also may be substrates for LBO.

Then, these HO-CL derivatives were incubated with recombinant LBO proteins as potential substrates. 4- and 16-HO-MeCLAs, but not other HO-CL derivatives, were consumed by LBO. Although we searched for LBO products of 4- and 16-HO-MeCLAs with the

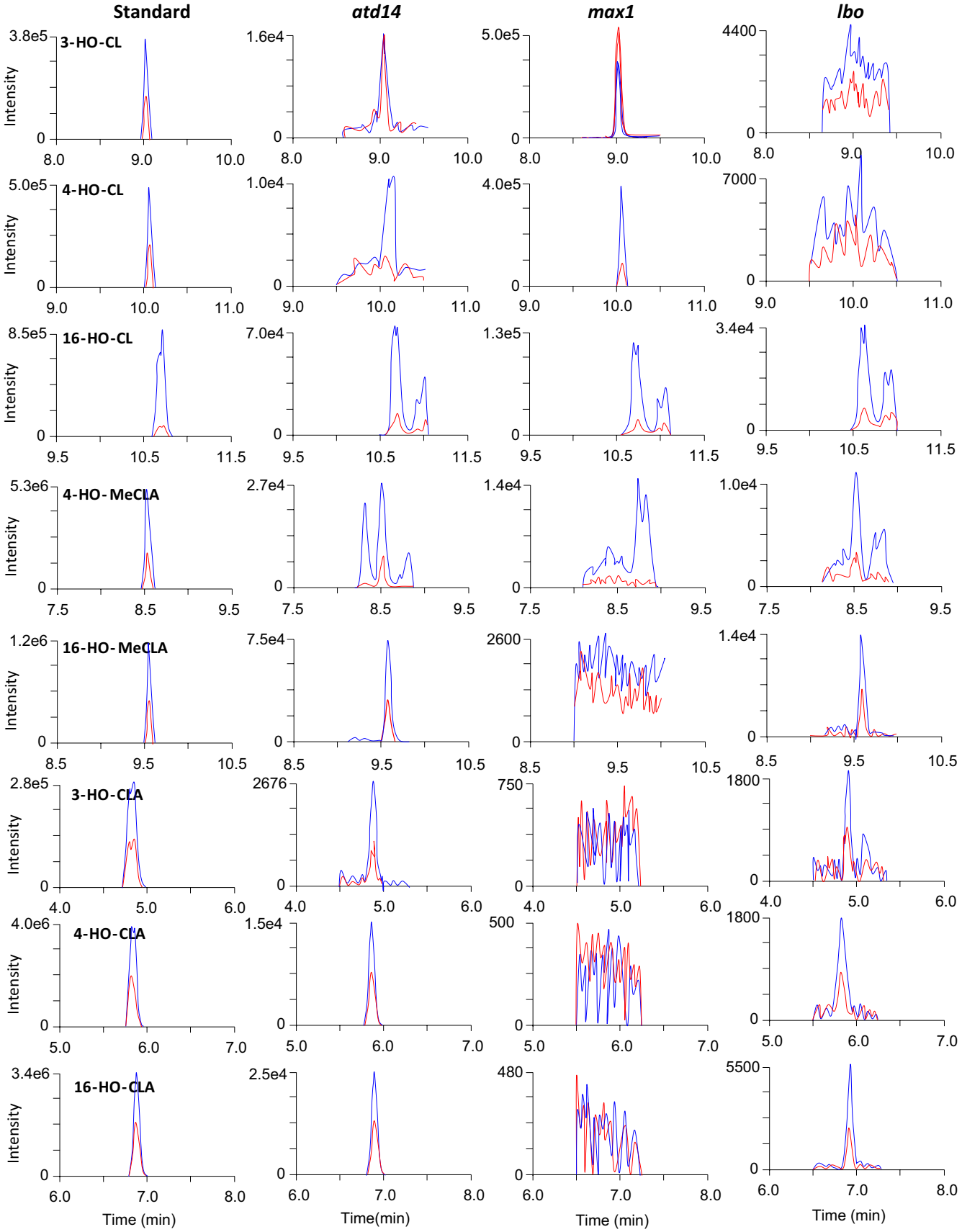
Standard
atd14
max1
lbo
3-HO-CL
4-HO-CL
16-HO-CL
4-HO-MeCLA
16-HO-MeCLA
3-HO-CLA
4-HO-CLA
16-HO-CLA
Intensity
Time (min)
Time(min)

FIGURE 8 Identification of endogenous HO-CLs, HO-CLAs, and HO-MeCLAs in basal parts of shoot tissues of *atd14* mutants, *max1* mutants, and *lbo* mutants. 3-, 4-, and 16-HO-CLs appeared to accumulate in *max1* mutants and 4-, and 16-HO-MeCLA in *lbo* mutants. MRM chromatograms of 3-HO-CL (blue, 301.0/97.0; red, 319.0/205.0; *m/z* in positive mode), 4-HO-CL (blue, 301.0/97.0; red, 301.0/148.0; *m/z* in positive mode), 16-HO-CL (blue, 301.0/97.0; red, 301.0/189.0; *m/z* in positive mode), 4-HO-MeCLA (blue, 345.0/97.0; red, 345.0/216.0; *m/z* in positive mode), 16-HO-MeCLA (blue, 345.0/97.0; red, 363.0/97.0; *m/z* in positive mode), and 3-, 4-, and 16-HO-CLA (blue, 347.0/113.0; red, 347.0/69.0; *m/z* in negative mode) are shown

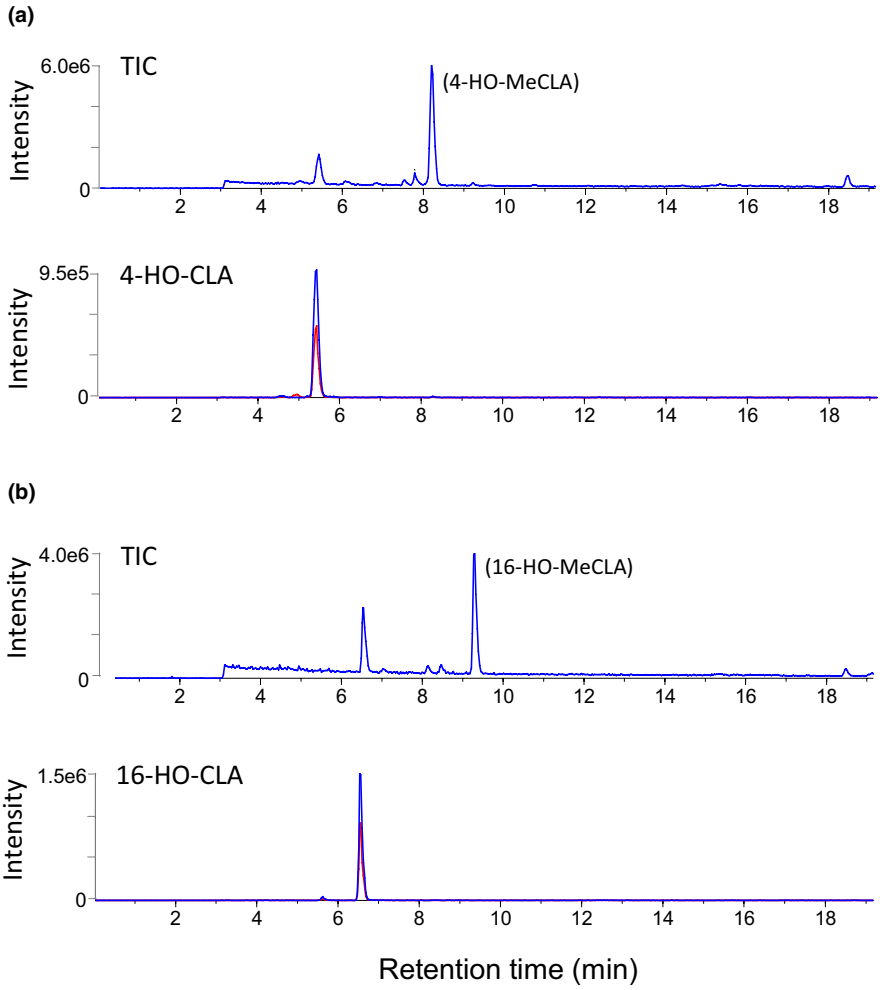

FIGURE 9 Recombinant LBO proteins convert 4- and 16-HO-MeCLA mainly into the corresponding HO-CLAs. Each substrate was incubated for 15 min. The extracts were analyzed by LC-MS/MS with the D-ring fragment (*m/z* 97) as an indicator to identify the metabolites from each HO-CLA-fed LBO. Total ion and MRM chromatograms of HO-CLAs (blue, 347.0/113.0; red, 347.0/69.0; *m/z* in negative mode) are shown

D-ring fragment (*m/z* 97) as an indicator by LC-MS/MS, we could not find any candidates for LBO products (Figure 9). As in the case of MeCLA, the corresponding HO-CLA was detected as a major reaction product.

4 | DISCUSSION

This study of LBO function has led to expansion of the list of strigolactone-like compounds in *Arabidopsis* to now include CLs (3-HO-CL, 4-HO-CL, 16-HO-CL), CLAs (3-HO-CLA, 4-HO-CLA, 16-HO-CLA), MeCLAs (4-HO-MeCLA, 16-HO-MeCLA), and 1'-HO-MeCLA (Figures 1 and 7). All were detected in *Arabidopsis* plants, but CLAs were not detected in *max1* mutants. CLAs and MeCLAs were detected in *lbo* mutants, but not 1'-HO-MeCLA. Heterologously expressed MAX1 protein could convert all CLs to equivalent CLAs. Heterologous LBO protein consumed MeCLA, 4-HO-MeCLA, and 16-HO-MeCLA. LBO produced some 1'-HO-MeCLA from MeCLA. Deuterated substrate feeding demonstrated that the previously described product of LBO, [MeCLA + 16 Da], is 1'-HO-MeCLA. These data support LBO acting downstream of MAX1 and MeCLA to produce 1'-HO-MeCLA (Figure 1). However, further experimentation is required to confirm MeCLA as a direct substrate of LBO *in planta*.

1'-HO-MeCLA was also produced by MeCLA-fed maize, tomato, and sorghum LBO proteins, suggesting that conversion of MeCLA into 1'-HO-MeCLA may occur *in planta* and may be conserved among different seed plant species.

Then, the question arises whether 1'-HO-MeCLA is a biologically important SL or not. The synthetic standard for 1'-HO-MeCLA is not yet available and the yield of 1'-HO-MeCLA by LBO protein reaction is too low to obtain enough for shoot branching assays. As the substitution of 1'-HO-MeCLA is very unstable and could

be readily converted, it is possible that 1'-HO-MeCLA is a precursor for an unknown, downstream shoot branching inhibitor(s) and a subsequent unknown enzyme(s) converts 1'-HO-MeCLA into the true shoot branching inhibitor(s). We will continue to search for any candidate compounds that are likely to be derived from 1'-HO-MeCLA from *atd14* mutants. *LBO* was uncovered from transcriptomics (Brewer et al., 2016), and similar methods recently led to the discovery that CYP722C from cowpea and tomato converts CLA directly to orobanchol (Wakabayashi et al., 2019) and that a 2-oxoglutarate-dependent dioxygenase (2-OGD) from a nearby clade to *LBO* is involved in SL biosynthesis in *Lotus japonicus* (Mori, Nomura, & Akiyama, 2020). We will continue reverse genetic and mass spectrometric approaches to find related SL biosynthetic genes and shoot branching inhibitors. CLA seems to be a key precursor for canonical SLs. We will test how LBO relates to CLA and canonical SLs by identifying *lbo* mutants from plants that produce canonical SLs.

It is important to note that the LBO protein assay produced much more CLA from MeCLA than 1'-HO-MeCLA. It is possible that CLA is a non-enzymatic by-product of 1'-HO-MeCLA formed under our reaction conditions. In addition, the high instability of 1'-HO-MeCLA compared to CLA probably greatly under-represents the true production amount of 1'-HO-MeCLA. On the other hand, *O*-demethylations have been reported for 2-OGDs, thebaine 6-*O*-demethylase and codeine *O*-demethylase, catalyzing *O*-demethylation in the final steps of morphine biosynthesis (Hagel & Facchini, 2010). Therefore, we cannot exclude the possibility that the main function of LBO in plants involves demethylation of MeCLA and that 1'-HO-MeCLA is just an intermediate for demethylation. This is somewhat difficult to reconcile with our previous result that showed that CLA was detected from *lbo* mutants, but not from its wild type (Brewer et al., 2016), indicating that CLA accumulates in *lbo* mutants. A methyltransferase is proposed to be involved in conversion from CLA into MeCLA and should be functional in *lbo* mutants. Thus, CLA would not be expected to accumulate in *lbo* mutants unless the methyltransferase was somehow downregulated. Identification of the methyltransferase should help to clarify the meaning of methylation and demethylation in the production of shoot branching inhibitors.

lbo-2 mutants with a point mutation in the predicted catalytic domain display extra shoot branching. The present study demonstrated that recombinant LBO-2 protein is very weak at converting MeCLA into 1'-HO-MeCLA (Figure 5). In contrast, LBO-3 appears to have normal function in our assay (Figure 5). The shoot branching phenotype of *lbo-3* mutants with a point mutation elsewhere in the gene is much weaker than *lbo-2* and only just significantly more than wild type (Brewer et al., 2016). It is possible that the protocol was not sensitive enough to observe subtle defects in reaction efficiency. Alternatively, the LBO-3 mutation may reveal an unknown protein functional or interaction domain at the mutation site, which only affects its bioactivity *in planta*. It may be useful to test LBO and LBO-3 in combination with other SL biosynthesis enzymes as they become discovered.

In addition to 1'-HO-MeCLA, other unstable, non-canonical SLs were found in the basal parts of shoot tissues (Figure 8). So far, identification of SLs has been mainly conducted from root tissues and this is the first report to show that SLs exist in basal parts of shoots of *Arabidopsis*. There were no apparent differences in SL levels between the two tissues when peak areas were compared (Figure 4). In contrast, levels of SLs are very low or undetectable from shoot of sorghum (Yoneyama et al., 2007) and rice plants (Umehara, Hanada, Magome, Takeda-Kamiya, & Yamaguchi, 2010). *Arabidopsis* could be quite particular in containing the same levels of SLs in the basal part of shoot and root tissues. Perhaps this is because *Arabidopsis* is a non-host of AM fungi. Even though *Arabidopsis* was reported to produce orobanchol (Goldwasser, Yoneyama, Xie, & Yoneyama, 2008;Kohlen et al., 2011), a canonical SL that is widely distributed in the plant kingdom (Yoneyama et al., 2008, 2011), we could detect neither orobanchol nor any other known canonical SLs from *Arabidopsis* tissues. Non-canonical SLs seem to be predominant in *Arabidopsis* and may not be released into the soil because *Arabidopsis* does not need to attract AM fungi to form a relationship with them. However, there are hints that SLs in *Arabidopsis* may promote interaction with other beneficial soil fungi (Carvalhais et al., 2019). So, there is likely much more to learn on that topic.

As summarized in Figure 7, MAX1 oxidizes C-19 methyl group to carboxylic acid not only in CL, but also in HO-CLs in *Arabidopsis* plants. Baz et al. (2018) also detected 3-HO-CL from rice *d14* mutant roots and demonstrated that 9-*cis*-3-HO-β-apo-10'-carotenal-fed to OsCCD8 is converted into 3-HO-CL. These results suggest that HO-CLs are also converted by MAX3 from HO-carotenal. The *Arabidopsis* MAX1 enzyme has the ability to convert 2-HO-CL and 18-HO-CL into respective HO-CLAs. However, these HO-CL derivatives could not be found from *Arabidopsis* plants. It is intriguing why *Arabidopsis* produces such various and particular HO-CL derivatives.

5 | CONCLUSION

Deciphering the whole SL biosynthetic pathway and characterization of yet unidentified biosynthetic intermediates is essential for devising new strategies to regulate the multiple functions of SLs through manipulation of SL production and exudation, both quantitatively and qualitatively. It should be noted that SL production and exudation vary with plant species (even between cultivars or genotypes of the same plant species), growth conditions, and growth stages. In the present study, we have progressed with potential enzymatic functions of LBO and MAX1 and their substrates and products downstream of CL in the SL biosynthetic pathway in *Arabidopsis*. As most seed plant species sequenced so far contain a single *LBO* gene, and the *LBO* gene lineage appears to have been derived deep in plant evolutionary history (Walker, Siu-Ting, Taylor, O'Connell, & Bennett, 2019), the biological function of LBO is likely to be highly conserved in the plant kingdom.

ACKNOWLEDGMENTS

We would like to thank Nozomi Nanai for technical assistance. This study was supported by the Japan Science and Technology Research

Promotion Program for Agriculture, Forestry, Fisheries and Food Industry, the Japan Society for the Promotion of Sciences (KAKENHI 15K07093, 16K07618, 16K18560, 17K07650), the Japan Science and Technology Agency PRESTO (JPMJPR17QA) and the Australian Research Council (DP110100808, FT180100081).

CONFLICT OF INTEREST

The authors declare no conflict of interest associated with the work described in this article.

AUTHOR CONTRIBUTIONS

Kaori Yoneyama, K.A., Koichi Yoneyama, and T.N. designed the research. Kaori Yoneyama, K.A., N.M., X.X., and P.B. performed research. Kaori Yoneyama, K.A., H.N., S.H., S.Y., M.U., and C.B. analyzed data. Kaori Yoneyama, K.A, and P.B. wrote the manuscript.

REFERENCES

Abe, S., Sado, A., Tanaka, K., Kisugi, T., Asami, K., Ota, S., … Nomura, T. (2014). Carlactone is converted to carlactonoic acid by MAX1 in *Arabidopsis* and its methyl ester can directly interact with AtD14 in vitro. *Proceedings of the National Academy of Sciences of the United States of America*, *111*(50), 18084–18089. https://doi.org/10.1073/pnas.1410801111

Akiyama, K., Matsuzaki, K., & Hayashi, H. (2005). Plant sesquiterpenes induce hyphal branching in arbuscular mycorrhizal fungi. *Nature*, *435*(7043), 824–827. https://doi.org/10.1038/nature03608

Al-Babili, S., & Bouwmeester, H. J. (2015). Strigolactones, a novel carotenoid-derived plant hormone. *Annual Review of Plant Biology*, *66*(1), 161–186. https://doi.org/10.1146/annurev-arplant-043014-114759

Alder, A., Jamil, M., Marzorati, M., Bruno, M., Vermathen, M., Bigler, P., … Al-Babili, S. (2012). The path from β-carotene to carlactone, a strigolactone-like plant hormone. *Science*, *335*(6074), 1348–1351. https://doi.org/10.1126/science.1218094

Baz, L., Mori, N., Mi, J., Jamil, M., Kountche, B. A., Guo, X., … Al-Babili, S. (2018). 3-Hydroxycarlactone, a novel product of the strigolactone biosynthesis core pathway. *Molecular Plant*, *11*(10), 1312–1314. https://doi.org/10.1016/j.molp.2018.06.008

Brewer, P. B., Yoneyama, K., Filardo, F., Meyers, E., Scaffidi, A., Frickey, T., … Beveridge, C. A. (2016). *LATERAL BRANCHING OXIDOREDUCTASE* acts in the final stages of strigolactone biosynthesis in *Arabidopsis*. *Proceedings of the National Academy of Sciences of the United States of America*, *113*(22), 6301–6306. https://doi.org/10.1073/pnas.1601729113

Carvalhais, L. C., Rincon-Florez, V. A., Brewer, P. B., Beveridge, C. A., Dennis, P. G., & Schenk, P. M. (2019). The ability of plants to produce strigolactones affects rhizosphere community composition of fungi but not bacteria. *Rhizosphere*, *9*, 18–26. https://doi.org/10.1016/j.rhisph.2018.10.002

Charnikhova, T. V., Gaus, K., Lumbroso, A., Sanders, M., Vincken, J.-P., De Mesmaeker, A., … Bouwmeester, H. J. (2018). Zeapyranolactone – A novel strigolactone from maize. *Phytochemistry Letters*, *24*, 172–178. https://doi.org/10.1016/j.phytol.2018.01.003

Charnikhova, T. V., Gaus, K., Lumbroso, A., Sanders, M., Vincken, J.-P., De Mesmaeker, A., … Bouwmeester, H. J. (2017). Zealactones. Novel natural strigolactones from maize. *Phytochemistry*, *137*, 123–131. https://doi.org/10.1016/j.phytochem.2017.02.010

Cook, C. E., Whichard, L. P., Turner, B., Wall, M. E., & Egley, G. H. (1966). Germination of witchweed (*Striga lutea* Lour.): Isolation and properties of a potent stimulant. *Science*, *154*(3753), 1189–1190. https://doi.org/10.1126/science.154.3753.1189

Goldwasser, Y., Yoneyama, K., Xie, X., & Yoneyama, K. (2008). Production of strigolactones by *Arabidopsis thaliana* responsible for *Orobanche aegyptiaca* seed germination. *Plant Growth Regulation*, *55*(1), 21–28. https://doi.org/10.1007/s10725-008-9253-z

Gomez-Roldan, V., Fermas, S., Brewer, P. B., Puech-Pagès, V., Dun, E. A., Pillot, J.-P., … Rochange, S. F. (2008). Strigolactone inhibition of shoot branching. *Nature*, *455*(7210), 189–194. https://doi.org/10.1038/nature07271

Hagel, J. M., & Facchini, P. J. (2010). Dioxygenases catalyze the *O*-demethylation steps of morphine biosynthesis in opium poppy. *Nature Chemical Biology*, *6*, 273. https://doi.org/10.1038/nchembio.317

Kohlen, W., Charnikhova, T., Liu, Q., Bours, R., Domagalska, M. A., Beguerie, S., … Ruyter-Spira, C. (2011). Strigolactones are transported through the xylem and play a key role in shoot architectural response to phosphate deficiency in nonarbuscular mycorrhizal host Arabidopsis. *Plant Physiology*, *155*(2), 974–987. https://doi.org/10.1104/pp.110.164640

Mori, N., Nishiuma, K., Sugiyama, T., Hayashi, H., & Akiyama, K. (2016). Carlactone-type strigolactones and their synthetic analogues as inducers of hyphal branching in arbuscular mycorrhizal fungi. *Phytochemistry*, *130*, 90–98. https://doi.org/10.1016/j.phytochem.2016.05.012

Mori, N., Nomura, T., & Akiyama, K. (2020). Identification of two oxygenase genes involved in the respective biosynthetic pathways of canonical and non-canonical strigolactones in *Lotus japonicus*. *Planta*, *251*(2), 40. https://doi.org/10.1007/s00425-019-03332-x

Motonami, N., Ueno, K., Nakashima, H., Nomura, S., Mizutani, M., Takikawa, H., & Sugimoto, Y. (2013). The bioconversion of 5-deoxystrigol to sorgomol by the sorghum, *Sorghum bicolor* (L.). *Moench*. *Phytochemistry*, *93*, 41–48. https://doi.org/10.1016/j.phytochem.2013.02.017

Nomura, T., Kushiro, T., Yokota, T., Kamiya, Y., Bishop, G. J., & Yamaguchi, S. (2005). The last reaction producing brassinolide is catalyzed by cytochrome P-450s, CYP85A3 in tomato and CYP85A2 in *Arabidopsis*. *Journal of Biological Chemistry*, *280*(18), 17873–17879. https://doi.org/10.1074/jbc.M414592200

Nomura, T., Magome, H., Hanada, A., Takeda-Kamiya, N., Mander, L. N., Kamiya, Y., & Yamaguchi, S. (2013). Functional analysis of *Arabidopsis* CYP714A1 and CYP714A2 reveals that they are distinct gibberellin modification enzymes. *Plant and Cell Physiology*, *54*(11), 1837–1851. https://doi.org/10.1093/pcp/pct125

Seto, Y., Sado, A., Asami, K., Hanada, A., Umehara, M., Akiyama, K., & Yamaguchi, S. (2014). Carlactone is an endogenous biosynthetic precursor for strigolactones. *Proceedings of the National Academy of Sciences of the United States of America*, *111*(4), 1640–1645. https://doi.org/10.1073/pnas.1314805111

Tanaka, K., Struts, A. V., Krane, S., Fujioka, N., Salgado, G. F. J., Martínez-Mayorga, K., … Nakanishi, K. (2007). Synthesis of CD_3-labeled 11-*cis*-retinals and application to solid-state deuterium NMR spectroscopy of rhodopsin. *Bulletin of the Chemical Society of Japan*, *80*(11), 2177–2184. https://doi.org/10.1246/bcsj.80.2177

Umehara, M., Hanada, A., Magome, H., Takeda-Kamiya, N., & Yamaguchi, S. (2010). Contribution of strigolactones to the inhibition of tiller bud outgrowth under phosphate deficiency in rice. *Plant and Cell Physiology*, *51*(7), 1118–1126. https://doi.org/10.1093/pcp/pcq084

Umehara, M., Hanada, A., Yoshida, S., Akiyama, K., Arite, T., Takeda-Kamiya, N., … Yamaguchi, S. (2008). Inhibition of shoot branching by new terpenoid plant hormones. *Nature*, *455*(7210), 195–200. https://doi.org/10.1038/nature07272

Wakabayashi, T., Hamana, M., Mori, A., Akiyama, R., Ueno, K., Osakabe, K., … Sugimoto, Y. (2019). Direct conversion of carlactonoic acid to orobanchol by cytochrome P450 CYP722C in strigolactone biosynthesis. *Science Advances*, *5*(12), eaax9067. https://doi.org/10.1126/sciadv.aax9067

Walker, C. H., Siu-Ting, K., Taylor, A., O'Connell, M. J., & Bennett, T. (2019). Strigolactone synthesis is ancestral in land plants, but canonical strigolactone signalling is a flowering plant innovation. *BMC Biology*, *17*(1), 70. https://doi.org/10.1186/s12915-019-0689-6

Xie, X., Kisugi, T., Yoneyama, K., Nomura, T., Akiyama, K., Uchida, K., … Yoneyama, K. (2017). Methyl zealactonoate, a novel germination stimulant for root parasitic weeds produced by maize. *J. Pestic. Sci.*, *42*(2), 58–61. https://doi.org/10.1584/jpestics.D16-103

Yoneyama, K., Mori, N., Sato, T., Yoda, A., Xie, X., Okamoto, M., … Nomura, T. (2018). Conversion of carlactone to carlactonoic acid is a conserved function of MAX1 homologs in strigolactone biosynthesis. *New Phytologist*, *218*(4), 1522–1533. https://doi.org/10.1111/nph.15055

Yoneyama, K., Xie, X., Kisugi, T., Nomura, T., Sekimoto, H., Yokota, T., & Yoneyama, K. (2011). Characterization of strigolactones exuded by Asteraceae plants. *Plant Growth Regulation*, *65*(3), 495–504. https://doi.org/10.1007/s10725-011-9620-z

Yoneyama, K., Xie, X., Kusumoto, D., Sekimoto, H., Sugimoto, Y., Takeuchi, Y., & Yoneyama, K. (2007). Nitrogen deficiency as well as phosphorus deficiency in sorghum promotes the production and exudation of 5-deoxystrigol, the host recognition signal for arbuscular mycorrhizal fungi and root parasites. *Planta*, *227*(1), 125–132. https://doi.org/10.1007/s00425-007-0600-5

Yoneyama, K., Xie, X., Sekimoto, H., Takeuchi, Y., Ogasawara, S., Akiyama, K., … Yoneyama, K. (2008). Strigolactones, host recognition signals for root parasitic plants and arbuscular mycorrhizal fungi, from Fabaceae plants. *New Phytologist*, *179*(2), 484–494. https://doi.org/10.1111/j.1469-8137.2008.02462.x

SUPPORTING INFORMATION

Additional supporting information may be found online in the Supporting Information section.

How to cite this article: Yoneyama K, Akiyama K, Brewer PB, et al. Hydroxyl carlactone derivatives are predominant strigolactones in *Arabidopsis*. *Plant Direct*. 2020;4:1–14. https://doi.org/10.1002/pld3.219